MATCH
Communications in Mathematical and in Computer Chemistry

MATCH Commun. Math. Comput. Chem. **80** (2018) 835-852

ISSN 0340 - 6253

Energy of Graphs and Remote Graphs in Hypercubes, Rhombellanes and Fullerenes

Mircea V. Diudea[a*], Atena Pîrvan–Moldovan[a], Raluca Pop[b], Mihai Medeleanu[c*]

[a]*Department of Chemistry, Faculty of Chemistry and Chemical Engineering, Babes-Bolyai University, 400028 Cluj, Romania, diudea@chem.ubbcluj.ro*

[b]*Faculty of Pharmacy, University of Medicine and Pharmacy, "Victor Babes" E. Murgu Square 2, 300041 Timisoara, Romania*

[c]*University Politehnica of Timisoara, Faculty of Industrial Chemistry and Environmental Engineering, C. Telbisz Str. No. 6, 300001, Timisoara, Romania*

mihai.medeleanu@upt.ro

(Received April 7, 2017)

Abstract

Energy of a graph is defined as the sum of absolute values of the eigenvalues of its adjacency matrix. Remote graphs are the graphs drawn on the remote adjacency matrices, built on the corresponding distance matrix by making unity a chosen distance *r* and zero the remaining entries. Energy of hypercubes, their remote graphs and hypercube derivatives made on the tetrahedron were computed; results were rationalized and analytical formulas derived. Rhombellanes form a class of multi-shell rhombic polytopes, of which vertices are *k*-partite. This property facilitated identification of partitions as polyhedra and evaluation of their graph energy. A stabilization energy was calculated for the parent graphs with respect to their independent partitions, by analogy with the quantum computations in molecular graphs. Energy of C_{40} fullerenes and their remote graphs was computed and used in a QSPR study to predict the total energy per atom, computed at the Hartree-Fock level of theory. Ability of graph energy to approach the quantum computed energy is discussed in connection with other topological descriptors.

1 Introduction

A *graph* $G(V,E)$ is a pair of two sets, V and E, $V=V(G)$ being a finite nonempty set and $E=E(G)$ a binary relation defined on V [1]. Any graph can be expressed in terms of pertinent order, real, symmetric matrices, the simplest one being the adjacency A matrix; its entries are either 1 if $i \neq$ j and $(i, j) \in E(G)$, or 0 if $i = j$ or $(i, j) \notin E(G)$.

Remote graphs are the graphs drawn on the remote adjacency matrices, built on the corresponding distance matrix by making unity a chosen distance r and zero the remaining entries [2,3]. The half sum of entries in A_2 and A_3 matrices represents the well-known Gordon-Scantlebury [4] or Bertz [5] index and Polarity number [6], respectively. In the above, A_2 and A_3 represent the adjacency at two edge and three edge distance, respectively.

Cartesian product $G \times H$ of two graphs G and H, is a new graph having the vertex set $V(G \times H) = V(G) \times V(H)$, that is, every vertex of $G \times H$ is an ordered pair (u,v), where $u \in V(G)$ and $v \in V(H)$; two distinct vertices (u,v) and (x,y) are adjacent in $G \times H$ if either: $u = x$ and $vy \in E(H)$, or $v = y$ and $ux \in E(G)$.

Spectral graph theory is a field where graph theory and matrix theory meet with the Hückel approach of molecular π-energy. It is focused on the set of eigenvalues (and eigenvectors), called the spectrum of a (chosen) graph matrix.

Energy of a graph is defined as the sum of the absolute values of the eigenvalues of the chosen matrix [7]. The most studied is the adjacency matrix A and the related characteristic polynomial [8,9]

Hückel molecular orbital (HMO) method [10] is a simple Linear Combination of Atomic Orbitals LCAO for the calculation of energies in π-electron conjugated hydrocarbon systems, such as ethylene, butadiene or benzene. It is the theoretical basis for the Hückel's rule.

The energies of HMOs are just the eigenvalues of $A(G)$, or the roots of the characteristic polynomial**:**

$$Ch(G, \lambda) = \det|\lambda I - A| = \sum_k a_k (G) \lambda^{n-k}$$

The solutions λ_i : $i = 1, 2,.., n$ of $Ch(G, \lambda)$ represent the spectrum of the π- MO energies:

$$E_i = \alpha + \beta \lambda_i$$

Taking $\alpha = 0$ (the reference energy), and $\beta = 1$ (the unit energy), the energy of ith MO

$$E_i = \lambda_i$$

In Hückel theory, the *total π-electron energy* E_π (*i.e.*, the sum of energies of orbitals populated in the ground state) is calculated as:

$$E_\pi = \sum g_i \lambda_i$$

where g_i is the occupation number of the ith MO while λ_i, i = 1, 2,.., n are the eigenvalues of the molecular graph.

Spectrum of a graph, Spec(G), is the set of all roots λ_i, i = 1, 2,.., n of its characteristic polynomial or the eigenvalues of $A(G)$; they can be obtained, *e.g.*, by a diagonalization procedure. From the above, it is clear that the Hückel theory has a topological basis; HMOs are called sometimes "topological orbitals".

After the introductory part, the section 2 gives a summary information on the energy of hypercubes; the third section speaks about the remote graphs of hypercubes; section 4 introduces the "spongy" hypercubes; in section 5 a new class of rhombic polyhedra is proposed; section 6 deals with the evaluation of C_{40} fullerene energy by the graph energy; conclusions and references will close this paper.

2 Energy of hypercube graphs

Hypercube Q_n (or n-cube) is the graph whose vertex set V_n consists of $2n$ n-tuples with coordinates 0 or 1, where two vertices are adjacent if their respective vectors differ in exactly one coordinate [1].

The hypercube can be defined recursively: Q_1 is taken K_2 (*i.e.*, the complete graph on two vertices) and, for $n > 2$, $Q_n = Q_{n-1} \times K_2$, the Cartesian product of Q_{n-1} with K_2 [11]. It can be drawn as a Hasse diagram [12].

Hypercube is a regular polytope in the space of any number of dimensions [13]. The n-cube $\{4,3^{n-2}\}$ (by Schläfli symbols) [14] has as its dual the n-orthoplex $\{3^{n-2},4\}$. The number of k-cubes contained in an n-cube $Q_n(k)$ comes out from the binomial coefficients $(2k+1)^n$

$$Q_n(k) = 2^{n-k}\binom{n}{k}; \qquad k = 0,..,n-1$$

Hypercube is a regular graph of degree n, according to Balinski [15] theorem. It is also bipartite, *i.e.*, the vertex set of the graph can be partitioned into two subsets, such that, within each set no vertices are adjacent; it is a vertex-transitive graph.

The adjacency matrix of Q_n can be written, considering the recursive nature of Q_n and commutativity of the submatrices, as

$$\mathrm{A}_{Q_n} = \begin{pmatrix} \mathrm{A}_{Q_{n-1}} & \mathrm{I}_{Q_{n-1}} \\ \mathrm{I}_{Q_{n-1}} & \mathrm{A}_{Q_{n-1}} \end{pmatrix}$$

$\mathrm{I}_{Qn\text{-}1}$ is the $2^{(n-1)} \times 2^{(n-1)}$ identity matrix (corresponding to $Q_{n\text{-}1}$) [1]. Consequently, one can write a recursive formula for its *characteristic polynomial*.

$$\begin{aligned} &\det(A_{Q_n} - \lambda I_{Q_n}) = \det((A_{Q_{n-1}} - \lambda I_{Q_{n-1}})^2 - I_{Q_{n-1}}) \\ &= \det((A_{Q_{n-1}} - \lambda I_{Q_{n-1}}) - I_{Q_{n-1}})\det((A_{Q_{n-1}} - \lambda I_{Q_{n-1}}) + I_{Q_{n-1}}) \\ &= \det(A_{Q_{n-1}} - (\lambda+1) I_{Q_{n-1}})\det(A_{Q_{n-1}} - (\lambda-1) I_{Q_{n-1}}) \end{aligned}$$

The solutions of Q_n characteristic polynomial, *i.e.*, eigenvalues λ_k, forming a spectrum, are

$$\mathrm{Spec}(Q_n) = \{-n, -n+2, -n+4,.., n-4, n-2, n\}$$

where n is the vertex degree $d(v)$ of Q_n. According to the Frobenius theorem, the eigenvalues of a graph ranges between $-d(v)_{\max}$ and $+d(v)_{\max}$.

Since Q_n is the Cartesian product $Q_{n\text{-}1} \times K_2$, there is a theorem enabling the calculation of eigenvalues for a Cartesian product graph from the eigenvalues of its factors:

Theorem 1 [16]: Let G and H be two graphs having the eigenvalues $\lambda_1, \ldots, \lambda_m$ and $\mu_1, \ldots, \mu_n$, respectively. The $m{\cdot}n$ eigenvalues of the Cartesian product $G \times H$ are the sums $\lambda_i + \mu_j$, for $1 < i < m$ and $1 < j < n$.

As a consequence, the Cartesian product of two hypercubes is another hypercube: $Q_i \times Q_j = Q_{i+j}$. The multiplicities for the ordered eigenvalues of Q_n adjacency matrix are given by the binomial coefficients, as established by the theorem:

Theorem 2 [17]: For the sequence of $n + 1$ distinct eigenvalues $\lambda_0 < \lambda_1 < \ldots < \lambda_n$, of Q_n spectrum, the multiplicity $\mathrm{M}(\lambda_k)$ is $\binom{n}{k}$, where $0 < k < n$.

The multiplicities of the eigenvalues are identical to rows of Pascal's triangle. A compact formula for the graph energy of Q_n energy was given in ref. [18]:

$$E(Q_n) = \begin{cases} \dfrac{n+1}{2}\dbinom{n+1}{\frac{n+1}{2}}; \text{ for } n = \text{odd} \\ n\dbinom{n}{\frac{n}{2}}; \text{ for } n = \text{even} \end{cases}$$

3 Remote graphs of hypercubes Q_n

Remote graphs of hypercubes Q_n were generated from their remote adjacency matrices A_r, for n=3 to 8; r takes values from 1 (adjacency at distance 1, the usual adjacency) to n. The vertex degree d equals n [15] in Q_n and r = 1; for higher r-values, d varies, as shown in Table 1. If Q_n are regular n-dimensional polytopes, their remote graphs turn to semiregular (as in case r = 2, the objects being n-demicubes) and then to uniform polytopes. n-Demicubes are n-polytopes formed by alternation of n-hypercubes (resulting two copies of the halved n-cube graph). The demicube is identical to the regular tetrahedron; the demitesseract is identical to the regular 16-cell; the demipenteract is semiregular; higher terms are all uniform polytopes (*i.e.*, vertex-transitive). More about this subject the reader can find in refs. [13,19]. The last remote graph (*i.e.*, the graph built on the largest distances in the parent graph) is a collection of P_2 disconnected graphs; there are exactly $2^{(n-1)}$ such disjoint edges. In case n = even and r = -1, the remote graph is a copy of the parent graph, with a mirror "mr" spectrum; Table 1 includes the energy computed for both the parent hypercubes and their remote graphs. Fig. 1 illustrates the Penteract and two of its remote graphs. In Fig. 2 (left), the demicube is illustrated.

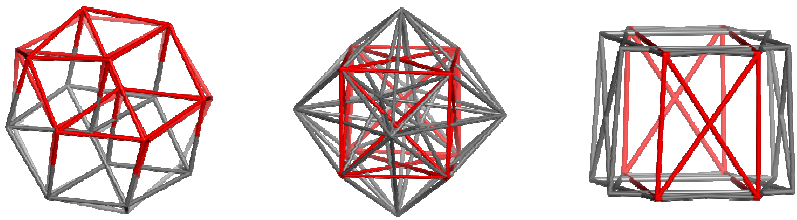

Q_5.32; d=5
Penteract

Q_5r_2.16; d=10
Demipenteract
5-Demicube

Q_5r_4.16; d=5
(two interlaced twisted cubes)

Figure 1. Remote graphs of Q_n; n=5.

Table 1. Q_n graph energy E_r of remote graphs (A_r; r=1 to n; vertex degree d)

n	8		7		6		5		4		3	
r	E_r	type	E_r	type	E_r	type	E_r	type	E_r	type	E_r	type
1	560	Q_8mr	280	Q_7mr	120	Q_6mr	60	Q_5mr	24	Q_4mr	12	Q_3mr
2	1008	2×d28	420	2×d21	180	2×d15	80	2×d10	24	2×d6	12	2×d3
3	1232	d56mr	560	d35mr	160	d20mr	80	d10mr	24	Q_4mr	8	4×e
4	1120	2×d70	560	2×d35	180	2×d15	60	2×d5	16	8×e		
5	1232	d 6mr	420	d21mr	120	Q_6mr	32	16×e				
6	1008	2×d28	280	2×d7	64	32×e						
7	560	Q_8mr	128	64×e								
8	256	128×e										
v	256		128		64		32		16		8	

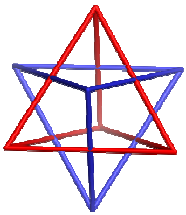

Q_3r_2.8
(demicube of Q_3)

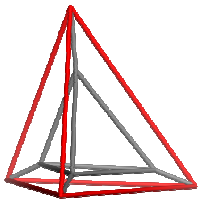

TQ_2.8

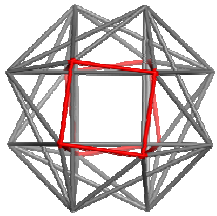

TQ_3r_2.16: 3^9; deg=7; e=56; f_3=48

Figure 2. Remote graphs of Q_n and TQ_n; n = 2; 3.

4 Spongy Hypercubes

Let us now take the graph $G(d,v)$ of a d-connected polyhedron on v-vertices and make n-times the Cartesian product with an edge; the operation results in a "spongy hypercube" $G(d,v,Q_{n+1}) = G(d,v)\square^n K_2$ (the square being another symbol for the Cartesian product). On each edge of the original polyhedral graph, a local hypercube Q_n will evolve; these hypercubes are incident in a hypervertex, according to the original degree, d. In a spongy hypercube, the original 2-faces are not be counted.

Conjecture. [20] *The k-facets of a spongy hypercube* $G(d,v,Q_n)$*, built on a 3-polytope with vertices of degree d, are combinatorially counted from the previous rank facets*

$$G(d,v,Q_n,k) = (v/n)\left[d \cdot n - (d-1)(n-k)\right] \cdot 2^{(n-k-1)} \cdot \binom{n}{k}; n > 1; k = 0,1,..n$$

The above formula represents the "embedding" of the hypercube on any polyhedron of vertex degree *d* (see the factor in the front of the almost classical hypercube counting), that transforms a cell in a hyper-multi-torus.

The alternating summation of the above counted facets accounts for the genus of the embedded surface:

$$\sum_{k=0}^{n} (-1)^k f_k = \chi(M) = 2(1-g); n > 1; k = 0,1,..n; g = f_2(G)/2$$

The "spongy" character of these structures comes from the genus *g* [1] of the hypersurface. Note that the summation ignores the (hyper) prisms evolved on each f_2 facets of the original cage. Since f_2 facets are not "seen", the dimension/rank [21-23] of spongy structures is counted from the rank of Q_n plus two: $k=n+2$.

Since the graph product is associative and commutative, we can write:

$$G(d,v,Q_{n+1}) = G(d,v)\square^n K_2 = G(d,v)\square Q_n = Q_n \square G(d,v)$$

Then, the eigenvalues of the spongy hypercubes can be calculated by summing the eigenvalues of Q_n and $G(d,v)$, cf. Theorem 1.

Analysis of numerical data obtained for the "spongy" TQ_n graphs and comparison with the formula obtained by Florkowski [18], enabled us to write the following formula for the graph energy:

$$E(TQ_n) = \begin{cases} \dfrac{n+3}{2}\dbinom{n+2}{\frac{n+3}{2}}; \text{for } n = \text{odd} \\ \dfrac{n+2}{2}\dbinom{n+2}{\frac{n+2}{2}}; \text{for } n = \text{even} \end{cases}$$

A detailed paper giving the way of finding of a general formula for the energy of TQ_n will be published elsewhere [24].

For the last remote adjacency A_n; n= diameter of G, a very simple formula was found:

$$E_n=3\times 2\hat{}n$$

coming out from the fact that the last remote graphs of TQ_n are (disjoint) 3-cubes, of which number is 2^(n-2). Data in this respect are given in Tables 2 and 3. Fig. 2 illustrates TQ_2.8 and a remote graph TQ_3r_2.16 (consisting in two interlaced twisted 3-cubes); it is a vertex transitive graph.

Table 2. TQ_n graph energy E_r at remote graphs (A_r; r = 1 to n); vertex degree d; no. disjoint Q_3 = 2^(n-2)

A_r	TQ_6		TQ_5		TQ_4		TQ_3		TQ_2		TQ_1	
	E_r	type	E_r	type	E_r	type	E_r	type	E_r	type	E_r	type
A_1	280	d=8	140	d=7	60	d=6	30	d=5	12	d=4	6	d=3
A_2	450	d=25	204	d=18	72	d=12	32	d=7	12	$1Q_3$		
A_3	480	d=40	208	d=22	72	d=10	24	$2Q_3$				
A_4	510	d=35	168	d=13	48	$4Q_3$						
A_5	360	d=16	96	$8Q_3$								
A_6	192	$16Q_3$										
v	120		64		32		16		8		4	

Table 3. Energy of the last remote graphs (disjoint Q_3) of TQ_n (cf. A_r ; r = diam; m=multiplicity); E_n=3×2^n.

TQ_n	TQ_6	TQ_5	TQ_4	TQ_3	TQ_2	TQ_1
v	128	64	32	16	8	4
λ	3	3	3	3	3	3
	1	1	1	1	1	-1
	-1	-1	-1	-1	-1	-1
	-3	-3	-3	-3	-3	-1
m	16	8	4	2	1	2^(n-2)
	48	24	12	6	3	3×2^(n-2)
	48	24	12	6	3	3×2^(n-2)
	16	8	4	2	1	2^(n-2)
E_n	192	96	48	24	12	

5 Rhombellanes

Rhombic polyhedra [25,26] represent aesthetic appeal objects, of mathematical interest. The best known is the Triacontahedron, a dual of the Archimedean Icosidodecahedron, denoted here Rh_{30}.32 (Fig. 3); the subscript is the number of rhombic faces while the last number counts the vertices in the graph.

A new class of multi-shell rhombic polytopes, called Rhombellanes, was proposed by Diudea [20]; they are tessellated by [1,1,1] Propellane, an organic molecule, first synthesized by Wiberg and Walker [27].

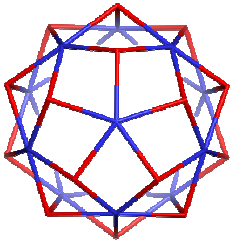	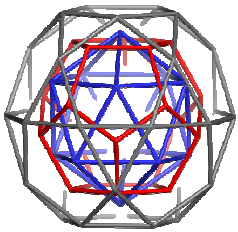
Rh_{30}.32	Icosahedron (blue); Dodecahedron (red) and Icosidodecahedron (gray)

Figure 3. Triacontahedron (left) and three disconnected polyhedra composing rhombellanes.

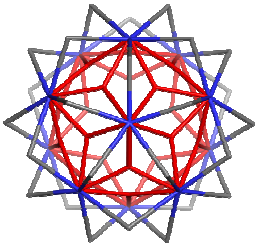

$rbl_1A(Rh_{30})$.62

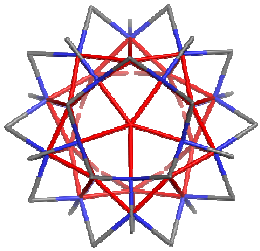

$rbl_1B(Rh_{30})$.62

Figure 4. Rhombellanes of the 1st generation.

Rhombellanes are built up by a procedure, we called “rhombellation”, achieved as follows. Join by a new point the vertices lying opposite diagonal in each rhomb of a Rh-cage to get rbl_1 generation (possible A and B isomers, as there are two diagonals – see Fig. 4). In a second step, put a new point opposite to a vertex of degree higher than 2 and join the new point with the vertices of $d = 2$ surrounding that vertex of $d > 2$, thus local Rh-cells being formed in the new structures rbl_2 (of generation 2 –see Fig. 5). The process can continue, in this way new shells/ generations being added to the parent object Since the two diagonals may be topologically different, each generation may consist of two isomers (denoted here as A and B, respectively).

All the rings in rhombellanes are rhombs. As a general property, all the vertex classes represent non-connected sets, thus the chromatic number equals the number of vertex classes. This property facilitates identification of vertex partitions as polyhedra and evaluation of their graph energy. A “binding” energy E_{bind} (in Beta units) can be calculated (see Table 4) for the parent graphs with respect to their independent partitions (*i.e.*, energy of composition, E_{compos}), by analogy with the quantum computations in molecular graphs.

$E_{bind} = E - E_{compos}$.

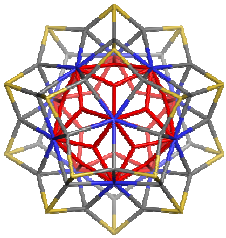

$rbl_2A(Rh_{30})$.82

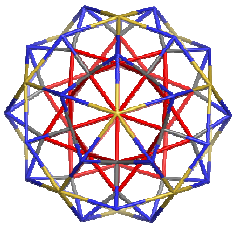

$rbl_2B(Rh_{30})$.74

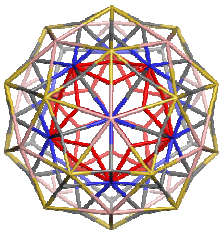

$rbl_3A(Rh_{30})$.94

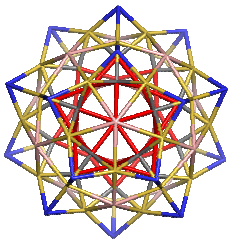

$rbl_3B(Rh_{30})$.94

Figure 5. Rhombellanes of the 2nd (top) and 3rd (bottom) generation.

Table 4. Rhombellanes related to Rh_{30}.32; Graph energy; $E_{bind} = E - E_{compos}$.

	Cluster	Composition	v	E	E_{compos}	E_{bind}	λ max	λ min
1	Icosahedron		12	23.416			5	-2.236
2	Dodecahedron		20	29.416			3	-2.236
3	Icosidodecahedron		30	55.416			4	-2
4	Rh_{30}	1+2	32	47.896	52.832	-4.936	3.873	-3.873
5	$rbl_1A(Rh_{30})$.62	1+2+3	62	71.872	108.248	-36.376	5	-5
6	$rbl_1B(Rh_{30})$.62	1+2+3	62	87.314	108.248	-20.934	4.583	-4.583
7	$rbl_2A(Rh_{30})$.82	1+2x2+3	82	129.43	137.664	-8.234	5.269	-5.269
8	$rbl_2B(Rh_{30})$.74	2x1+2+3	74	132.828	131.664	1.164	5	-5
9	$rbl_3A(Rh_{30})$.94	2x1+2x2+3	94	154.906	161.08	-6.174	5.568	-5.568
10	$rbl_3B(Rh_{30})$.94	2x1+2x2+3	94	162.292	161.08	1.212	5.349	-5.349

6 Graph energy in fullerene energy evaluation

Ordering of C_{40} fullerene graphs according to the molecular total energy was reported earlier, with respect to semiempirical [28] or higher theoretical level [29]. Pentagon fusion (calculated as the number of fused pentagonal faces n_p) was found the major destabilizing factor in the small classical fullerenes. The maximum value occurs for the hemidodecahedral capped isomer 40:1, and the minimum for the two isomers 40: 38 and 40: 39 (see Table 5). The parameter n_p represents just the coefficient in Omega polynomial [30] of the term at exponent unity.

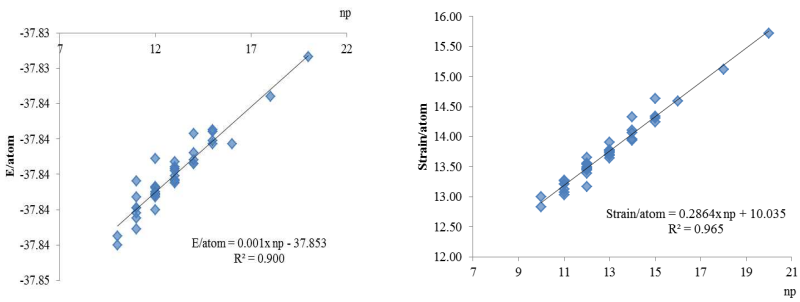

Figure 6. Plots of total energy/atom (in au - left) and strain energy/atom (in kcal/mol - right) vs the number of fused pentagons n_p.

The linear dependency of Hartree-Fock (6-31G*) energies of C_{40} isomers (in au - Table 5) vs. the parameter n_p was plotted in Figure 6 (left); it explains about 90 % of energy variance. A better dependence on n_p was shown by the strain energy (POAV1) [31,32], Figure 6 (right).

QSPR models can be derived in a variety of combinations; it is not the aim of this study to perform the best model to describe the quantum energy of C_{40}. Our goal was to show that the graph energy of these fullerenes (and others) can be used to evaluate the quantum calculated molecular energy.

Table 5. Total energy E_{tot} (HF(6-31G*; au)), strain (POAV1; kcal/mol) and topological parameters of C_{40} fullerenes (No. of fused pentagons n_p; Euclidean distance D3D; topological distance D; centrality index C(Sh(D)); energy of the parent graph E_1; sum of remote graphs energy per remote distance E_r; sum of remote graphs energy per square remote distance E_{rsq}; last eigenvalue LEig and the polarity number D3)

C_{40}	Sym	E_{tot} /atom	Strain /atom	n_p	D3D	D	C(Sh(D))	E_1	E_r	E_{rsq}	LEig	D_3
1	D_{5d}	-37.83	15.72	20	3178	3035	3.89	61.61	193.58	105.08	-2.80	29.51
2	C_2	-37.84	14.59	16	3128	3008	4.02	61.75	193.80	105.27	-2.73	30.63
3	D_2	-37.84	15.12	18	3146	3018	4.05	61.57	192.94	105.00	-2.76	30.43
4	C_1	-37.84	14.31	15	3111	3001	3.59	61.68	193.69	105.24	-2.68	30.78
5	C_s	-37.84	14.11	14	3108	2997	3.60	61.82	193.65	105.44	-2.69	30.85
6	C_1	-37.84	14.06	14	3102	2999	4.10	61.74	193.31	105.21	-2.67	30.97
7	C_s	-37.84	14.33	15	3102	2998	3.57	61.79	193.48	105.29	-2.68	30.97
8	C_{2v}	-37.84	14.63	15	3107	3002	4.13	61.64	191.39	104.65	-2.67	30.70
9	C_2	-37.84	13.77	13	3092	2995	3.54	61.63	193.56	105.10	-2.66	30.78
10	C_1	-37.84	13.73	13	3092	2995	3.57	61.76	193.88	105.37	-2.69	31.00
11	C_2	-37.84	14.25	15	3102	2997	3.60	61.60	193.34	105.07	-2.71	30.82
12	C_1	-37.84	13.68	13	3090	2997	3.47	61.74	194.92	105.48	-2.67	30.98
13	C_s	-37.84	13.75	13	3092	2998	4.04	61.80	194.48	105.46	-2.66	31.34
14	C_s	-37.84	13.56	12	3082	2995	3.43	61.82	195.32	105.60	-2.67	31.01
15	C_2	-37.84	13.49	12	3084	3001	3.36	61.73	195.39	105.45	-2.69	31.11
16	C_2	-37.84	13.69	13	3083	3001	3.39	61.62	194.60	105.16	-2.70	30.92
17	C_1	-37.84	13.64	13	3082	3000	3.38	61.70	195.27	105.44	-2.67	30.93
18	C_2	-37.84	13.94	14	3092	2999	3.38	61.69	194.90	105.39	-2.70	31.17
19	C_2	-37.84	13.90	13	3082	2998	3.45	61.79	195.24	105.55	-2.69	31.16

20	C_{3v}	-37.84	13.66	12	3087	3000	3.37	62.01	196.31	105.97	-2.69	31.23
21	C_2	-37.84	13.55	12	3087	2992	3.57	61.83	194.23	105.54	-2.68	31.34
22	C_1	-37.84	13.46	12	3086	2995	3.48	61.93	195.46	105.82	-2.67	31.40
23	C_2	-37.84	13.77	13	3092	2993	3.55	61.74	194.47	105.44	-2.67	31.38
24	C_s	-37.84	13.26	11	3078	2994	3.43	61.84	195.82	105.75	-2.63	31.30
25	C_2	-37.84	13.48	12	3083	2996	3.40	61.76	195.34	105.61	-2.68	31.25
26	C_1	-37.84	13.21	11	3077	2996	3.37	61.72	195.97	105.66	-2.64	31.21
27	C_2	-37.84	13.45	12	3079	2996	3.43	61.83	196.07	105.84	-2.66	31.28
28	C_s	-37.84	13.46	12	3086	2993	3.44	61.71	194.52	105.41	-2.66	31.39
29	C_2	-37.84	13.21	11	3074	2993	3.40	61.75	195.36	105.55	-2.65	31.02
30	C_3	-37.84	13.54	12	3077	2994	3.43	61.85	195.65	105.72	-2.67	31.12
31	C_s	-37.84	13.07	11	3074	2995	3.39	61.73	195.32	105.50	-2.63	30.93
32	D_2	-37.84	13.96	14	3095	3004	3.37	61.81	195.97	105.64	-2.70	31.52
33	D_{2h}	-37.84	14.33	14	3095	3004	3.79	61.89	195.16	105.46	-2.70	31.45
34	C_1	-37.84	13.39	12	3082	2997	3.37	61.76	195.83	105.71	-2.66	31.08
35	C_2	-37.84	13.27	11	3078	2999	3.36	61.77	196.06	105.69	-2.65	31.20
36	C_2	-37.84	13.12	11	3076	2997	3.37	61.78	196.39	105.80	-2.64	30.99
37	C_{2v}	-37.84	13.02	11	3078	2995	3.38	61.71	195.47	105.57	-2.64	31.10
38	D_2	-37.84	12.83	10	3071	2994	3.37	61.60	195.69	105.48	-2.63	30.87
39	D_{5d}	-37.84	13.00	10	3077	2990	3.38	61.58	193.92	105.16	-2.58	31.17
40	T_d	-37.84	13.17	12	3075	3000	3.40	61.82	195.46	105.61	-2.60	30.86

Table 6. Best models in describing total energy E_{tot}/atom.

X_1	X_2	X_3	R^2	St error
n_p			0.900	0.000662
$SD_{E/atom}$			0.849	0.000813
LEig			0.780	0.000981
D3D			0.777	0.000987
D			0.634	0.001266
C(Shell(D))			0.387	0.001638
E_r			0.309	0.001739
E_{rsq}			0.259	0.001801
E_1			0.026	0.002065

n_p	E_1		0.916	0.000616
	D_3		0.915	0.000617
	LEig		0.915	0.000617
	E_{rsq}		0.907	0.000645
	E_r		0.906	0.000650
n_p	E_1	LEig	0.924	0.000591
		D_3	0.921	0.000605
		C(Sh(D))	0.918	0.000614
$SD_{E/atom}$	LEig		0.897	0.000680
	D3D		0.882	0.000727
	C(Sh(D))		0.880	0.000735
	E_1		0.862	0.000787
	E_r		0.853	0.000814
$SD_{E/atom}$	LEig	C(Sh(D))	0.918	0.000615
		D3D	0.907	0.000655
		E_r	0.907	0.000656
		E_1	0.902	0.000673
		E_{rsq}	0.900	0.000678

Table 7. Best models in describing strain energy Strain/atom.

X_1	X_2	X_3	R^2	St error
n_p			0.965	0.112
D3D			0.879	0.209
SD_{Strain}			0.757	0.296
LEig			0.750	0.300
D (distance)			0.654	0.353
C(Sh(D))			0.536	0.409
n_p	C(Sh(D))		0.970	0.106
	E_1		0.968	0.109
	D_3		0.968	0.110
	E_r		0.967	0.110
	LEig		0.966	0.112
	D3D		0.965	0.113
n_p	C(Sh(D))	LEig	0.973	0.102
		E_1	0.972	0.102
		D_3	0.972	0.103
D3D	LEig		0.905	0.187
	D_3		0.891	0.200
	E_r		0.890	0.202
	E_{rsq}		0.887	0.204
	SD_{Strain}		0.885	0.2064
	E_1		0.884	0.2068
D3D	LEig	E_r	0.934	0.158
		E_{rsq}	0.926	0.168

Tables 6 and 7 list several combinations, including the energy of graphs and remote graphs, with and without the n_p parameter. A mention deserves the D3D descriptor as a steric descriptor that includes the n_p parameter in a hidden manner. A second mention is addressed to SD_E and SD_{Strain}, representing the "sum descriptors" computed as linear combinations of local descriptors in the "hypermolecule" algorithm developed by TOPO Group Cluj. This descriptor together with the last eigenvalue LEig and the other eigenvalues of graphs and/or remote graphs can satisfactory predict the quantum computed molecular energies of C_{40} fullerenes.

7 Conclusions

In this work, the adjacency matrix eigenvalues and graph energies were computed on hypercubes, spongy hypercubes, rhombellanes and the set of C_{40} fullerenes.

Data obtained for the "spongy" TQ_n graphs enabled us to write an analytical formula for calculating the graph energy of this class of graphs. The remote graphs, derived on the remote adjacency matrices of spongy hypercubes, deserve more exploring to find eventual hidden distance-based relations with the parent graphs.

Rhombellanes represent a new class of rhombic polytopes. In rhombellanes, a binding energy was calculated with respect to the vertex class partitions representing polyhedral cells.

Total energy (HF(6-31G*) and strain (POAV1) of the set of C40 fullerene was not particularly well described by the values of graph energy or remote graph energy. A better description was done by a topological parameter counting the fused pentagons within a fullerene isomer, eventually associated with other descriptors developed at Topo Group Cluj [33].

Acknowledgment: This work was supported by a grant of the Romanian National Authority for Scientific Research and Innovation, CCCDI – UEFISCDI, project number 8/2015, acronym GEMNS (under the frame of the ERA-NET EuroNanoMed II European Innovative Research and Technological Development Projects in Nanomedicine).

References

[1] F. Harary, *Graph Theory*, Addison–Wesely, Reading, 1969.

[2] P. E. John, M. V. Diudea, The second distance matrix of the graph and its characteristic polynomial, *Carpath. J. Math.* **20** (2004) 235–239.

[3] M. Rafailă, M. Medeleanu, C. Davidescu, M. V. Diudea, Laplacian and modified Laplacian matrices for quantification of chemical structures. *Studia Univ. Babes-Bolyai Chem.* **58** (2013) 51– 61.

[4] M. Gordon, G. R. Scantlebury, Nonrandom polycondensation: statistical theory of the substitution effect, *Trans. Faraday Soc.* **60** (1964) 604–621.

[5] S. H. Bertz, Branching in graphs and molecules, *Discr. Appl. Math.* **19** (1988) 65–83.

[6] H. Wiener, Structural determination of paraffin boiling points, *J. Am. Chem. Soc.* **69** (1947) 17–20.

[7] I. Gutman, The energy of graph, *Ber. Math. Statist. Sekt. Forschungsz. Graz* **103** (1978) 1–22.

[8] D. M. Cvetković, M. Doob, H. Sachs, *Spectra of Graphs*, Acad. Press, New York, 1980.

[9] X. Li, Y. Shi, I. Gutman, *Graph Energy*, Springer, New York, 2012.

[10] E. Hückel, Quantentheoretische Beiträge zum Benzolproblem. I. Die Elektronenkonfiguration des Benzols und verwandter Verbindungen, *Z. Phys.* **70** (1931) 204–286.

[11] G. Chartrand, P. Zhang, *Introduction to Graph Theory*, McGraw–Hill, Boston, 2005.

[12] K. A. Baker, P. Fishburn, F. S. Roberts, Partial orders of dimension 2, *Networks* **2** (1971) 11–28.

[13] H. S. M. Coxeter, *Regular Polytopes*, Dover, New York, 1973.

[14] L. Schläfli, Theorie der vielfachen Kontinuität Zürcher und Furrer, Zürich (Reprinted in: Ludwig Schläfli, 1814–1895, Gesammelte Mathematische Abhandlungen, Band 1, 167–387, Verlag Birkhäuser, Basel, 1950.

[15] M. L. Balinski, On the graph structure of convex polyhedra in n-space, *Pacific J. Math.* **11** (1961) 431–434.

[16] F. Harary, J. Hayes, H. Wu, A survey of the theory of hypercube graphs, *Comput. Math. Appl.* **15** (1988) 277–289.

[17] M. Cvetković, Spectrum of the graph of *n*-tuples, *Pub. Electrotech. Fac., Univ. Belgrade* **288** (1969) 91–95.

[18] S. F. Florkowski, Spectral graph theory of the hypercube; thesis, Naval postgraduate school, Monterey, California, http://hdl.handle.net/10945/3852, (2008–2012).

[19] T. Gosset, *On the Regular and Semi-Regular Figures in Space of n Dimensions*, Messenger Mathematics, Macmillan, 1900.

[20] M. V. Diudea, *Multi-Shell Polyhedral Clusters*, Springer, 2018.

[21] E. Schulte, Regular incidence-polytopes with Euclidean or toroidal faces and vertex-figures, *J. Comb. Theory A* **40** (1985) 305–330.

[22] E. Schulte, *Symmetry of Polytopes and Polyhedra. Handbook of Discrete and Computational Geometry*, Goodman & O'Rourke, 2004.

[23] E. Schulte, Polyhedra, complexes, nets and symmetry, *Acta Cryst.* **A70** (2014) 203–216.

[24] M. Saheli, M. V. Diudea, Energy of TQ_n, (2017), *in preparation*.

[25] I. Hafner, T. Zitko, Introduction to golden rhombic polyhedral, *Vis. Math.* **4** (2002a) #2(3).

[26] I. Hafner, T. Zitko, Relations among rhombic, Platonic and Archimedean solids, *Vis. Math.* **4** (2002b) #2(4).

[27] K. B. Wiberg, F. H. Walker, [1.1.1]Propellane, *J. Am. Chem. Soc.* **104** (1982) 5239–5240.

[28] M. Dinca, S. Ciger, M. Stefu, F. Gherman, K. Miklos, C.L. Nagy, O. Ursu, M.V. Diudea, Stability prediction in small fullerenes, *Carpath. J. Math.* **20** (2004) 211–221.

[29] E. Albertazzi, C. Domene, P. W. Fowler, T. Heine, G. Seifert, C. Van Alsenoy, F. Zerbetto, Pentagon adjacency as a determinant of fullerene stability, *Phys. Chem. Chem. Phys.* **1** (1999) 2913–2918.

[30] M. V. Diudea, Omega polynomial, *Carpath. J. Math.* **22** (2006) 43–47.

[31] R. C. Haddon, Rehybridization and π-orbital overlap in nonplanar conjugated organic molecules: π-Orbital axis vector (POAV) analysis and three-dimensional Hückel molecular orbital (3D-HMO) theory, *J. Am. Chem. Soc.* **109** (1987) 1676–1685.

[32] R. C. Haddon, Measure of nonplanarity in conjugated organic molecules: Which structurally characterized molecule displays the highest degree of pyramidalization? *J. Am. Chem. Soc.* **112** (1990) 3385–3389.

[33] O. Ursu, M. V. Diudea, TOPOCLUJ software program, Babes-Bolyai Univ., Cluj, 2005.